Nano-Structures & Nano-Objects 38 (2024) 101129

Contents lists available at ScienceDirect

Nano-Structures & Nano-Objects

journal homepage: www.elsevier.com/locate/nanoso

Unconventional eco-friendly synthesis of graphene and its electrochemical analysis

Muhammad Adeel Zafar [a], Yang Liu [b], Scarlett Allende [a], Mohan V. Jacob [a,*]

[a] Electronics Materials Lab, College of Science and Engineering, James Cook University, Townsville, QLD 4811, Australia
[b] College of Science and Engineering, James Cook University, Townsville, QLD 4811, Australia

ARTICLE INFO

Keywords:
Electrochemical behaviour
Graphene
Ascorbic acid
Uric acid
Dopamine
Atmospheric pressure microwave plasma
A sustainable precursor

ABSTRACT

In response to the growing demand for sustainable graphene synthesis methods, traditionally characterized by harsh conditions and prolonged processing, we present an innovative approach. Here, graphene is synthesized utilizing *melaleuca alternifolia*, a natural resource, under mild conditions of cold plasma. This method not only aligns with the increasing need for environmentally friendly processes but also boasts efficiency, producing graphene within seconds. Our investigation employs various analytical techniques, including Raman spectroscopy, confirming the successful synthesis of graphene. The distinctive peaks identified in the spectroscopic analysis validate the high quality of the graphene material produced. Beyond synthesis, our study delves into the electrochemical properties of the synthesized graphene. Rigorous testing with real biomolecules reveals enhanced current peaks, underscoring the potential applications of graphene in the realm of electrochemical sensing. This work contributes to advancing sustainable and efficient graphene synthesis while exploring its promising properties for practical applications.

1. Introduction

Graphene, celebrated for its exceptional properties, is typically synthesized using methods involving harsh conditions and non-renewable resources. The traditional approaches, including modified Hummers' method and chemical vapor deposition, present challenges such as environmental impact, extensive processing, and high costs [1,2]. Graphene has previously been synthesized using solution-based reduction methods, including photochemical, electrochemical, hydrothermal, and mechanochemical processes [3]. In response, the emerging atmospheric pressure microwave plasma (APMP) method offers a dry, sustainable, and scalable alternative for graphene synthesis. Unlike conventional methods, APMP eliminates the need for pre-heating, high vacuuming, and substrate dependence [4,5].

The choice of precursors significantly impacts sustainability. Commonly used non-renewable sources like graphite and graphene oxide are being replaced with regenerative alternatives. However, the use of sustainable precursors in APMP remains unexplored [6–9]. A potential solution lies in m*elaleuca alternifolia*, known as tea tree, a naturally occurring and hydrocarbon-rich resource. Cost-effective and abundant, it has shown promise for graphene synthesis. While previously used in the PE-CVD technique, the process was time-consuming and substrate-dependent [10,11]. The exploration of m*elaleuca alternifolia* in APMP for graphene synthesis could open new avenues for sustainable and efficient production. Furthermore, the utilization of such sustainably sourced graphene for the sensing of biomolecules including dopamine (DA), ascorbic acid (AA), and uric acid (UA) has may not been reported.

DA serves as a vital catecholamine neurotransmitter within the central nervous system, with its concentration typically measured in the range of 10 nM–1 μM in biological systems. Deviations from normal DA levels in biological fluids can serve as an indicative marker for various neurological diseases, including Parkinson's disease, schizophrenia, and HIV infection [12]. Similarly, UA is a product of purine metabolism, presenting itself within the range of 207–444 μM in the human body. Elevated or insufficient levels of UA may contribute to several illnesses such as kidney failure, gout, cardiovascular and chronic renal diseases, pneumonia, hyperuricemia, etc [13]. Moreover, AA stands out as one of the most essential vitamins in the human body, owing to its antioxidant properties. It acts as a protective agent for cells and tissues against oxidative stress, playing a crucial role in the metabolic processes of the human body. Under normal conditions, the intracellular concentration

* Corresponding author.
E-mail address: mohan.jacob@jcu.edu.au (M.V. Jacob).

https://doi.org/10.1016/j.nanoso.2024.101129
Received 21 December 2023; Received in revised form 20 February 2024; Accepted 29 February 2024
Available online 19 March 2024

of AA is estimated to be 1–2 mM. Abnormal levels of AA can lead to various illnesses within the central nervous system [12]. Notably, AA concentration generally surpasses the concentrations of DA and UA in biological systems. Consequently, the swift and accurate measurement of AA, DA, and UA concentrations in biological fluids is imperative for the clinical diagnosis of relevant diseases.

A wide range of methods has been used for the detection of these molecules. Among all those methods, electrochemical technique has the advantages of detecting molecules in a simple, fast and cost-effective way [14]. In the past, numerous studies were conducted for the electrochemical detection of DA, AA, and UA. Graphene has appealed scientists as an interesting material in the design of new electrochemical sensors owing to its high electro-catalytic activity, great conductivity and large surface area [15]. Graphene in its pristine form as well as its types including nitrogen-doped graphene/oxide [16], reduced-graphene oxide [17], or simply graphene oxide [18], and their composites with metals [19–21] have been employed for DA, AA, and UA detection. Graphene, synthesized particularly from a sustainable precursor has so far may not been reported for the electrochemical determination of DA, UA, and AA. It is crucial to use sustainable precursors since the depletion of the resources can put challenges for the future synthesis of graphene.

The current study aims to emphasize the feasibility of producing graphene from a sustainable source under mild conditions, such as low temperature and ambient environments. The research will elucidate the use of cold microwave plasma and define the optimal synthesis parameters utilized in the procedure. Additionally, we introduce the pioneering application of sustainably sourced graphene, derived from *melaleuca alternifolia* extract, for the electrochemical detection of DA, AA, and UA, signifying a notable advancement in this field.

2. Materials and methods

2.1. Materials

Tea tree oil was supplied by Australian Botanical Products (ABP, Victoria, Australia). Sodium dihydrogen orthophosphate, sodium hydroxide (NaOH), di-Sodium hydrogen orthophosphate, potassium chloride (KCl), potassium hexa-cyanoferrate (III) $K_3[Fe(CN)_6]$, DA. AA, and UA were procured from Sigma-Aldrich. Milli-Q ultrapure water was utilized throughout the experiments.

2.2. Synthesis of graphene

Graphene nanosheets were prepared in a downstream atmospheric pressure microwave plasma, employing a methodology outlined in a prior report [22,23]. The process involved introducing tea tree oil vapours into a plasma-ignited quartz chamber, with argon serving as the carrier gas. The tea tree oil vapours navigated through distinct plasma zones, undergoing a transformation into graphene. The extraction of graphene for subsequent analysis was carried out from the open end of the tube.

A critical exploration of the influential microwave power parameter was conducted across three discrete levels: 150 W, 200 W, and 250 W. This systematic investigation aimed to discern the optimal conditions for graphene synthesis. Following this, the process parameters were finely tuned, establishing 200 W as the optimal microwave power. This meticulous optimization of parameters not only contributes to the reproducibility of the synthesis process but also ensures enhanced control over the quality and characteristics of the synthesized graphene. In addition to the careful exploration of the influential microwave power parameter, the synthesis process was subjected to a comprehensive investigation of various other key parameters to refine and optimize the graphene production. Specifically, the effect of argon flow rate was scrutinized. The systematic variation and analysis of the argon flow rate proved to be a decisive factor in the graphene synthesis process. Extremes in flow rate, either excessively high or excessively low, resulted in the failure to synthesize graphene. After a series of rigorous experiments, the optimum condition was determined to be 3 standard liters per minute (slm) for the argon flow rate.

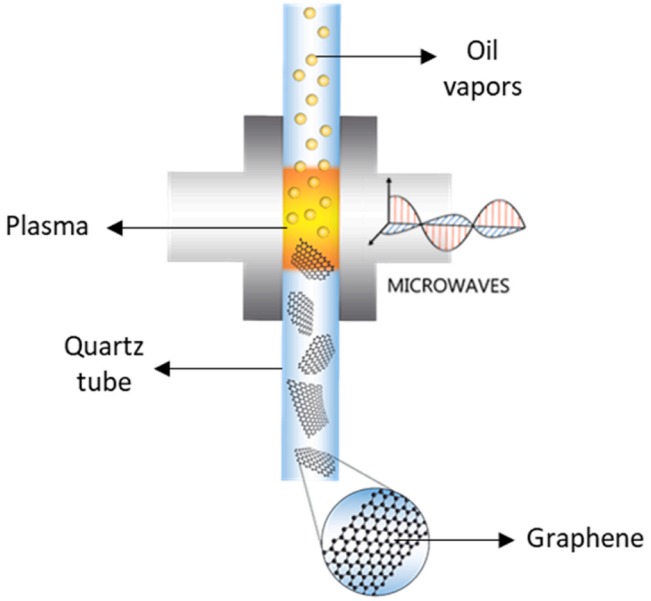

Fig. 1. Graphene fabrication scheme using downstream atmospheric pressure microwave plasma.

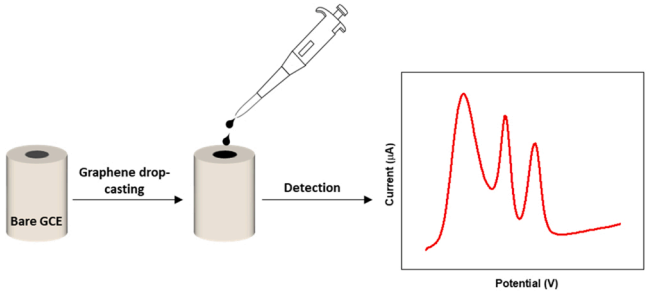

Fig. 2. Scheme for electrode preparation and detection.

Furthermore, the impact of synthesis time on the characteristics of the synthesized graphene was thoroughly examined. Different time intervals within the plasma environment were assessed to understand the temporal evolution of graphene properties. Overall, this multifaceted exploration of critical parameters, including microwave power, argon flow rate, and synthesis time, not only enhances our understanding of the synthesis process but also paves the way for establishing standardized and reproducible conditions for the scalable production of high-quality graphene nanosheets in downstream atmospheric pressure microwave plasma. The synthesis procedure is schematically shown in Fig. 1.

2.3. Electrode preparation

Prior to each testing or electrode modification, glassy carbon electrode (GCE) was passed through various cleaning stages, polishing using 0.3 μm and 0.05 μm alumina slurry, ultrasonication in ultrapure water as well as propanol solution. After cleaning, 10 μL of graphene aliquot (~1 mg/ml) was deposited on GCE and let it dry at atmospheric conditions. The scheme is shown in Fig. 2.

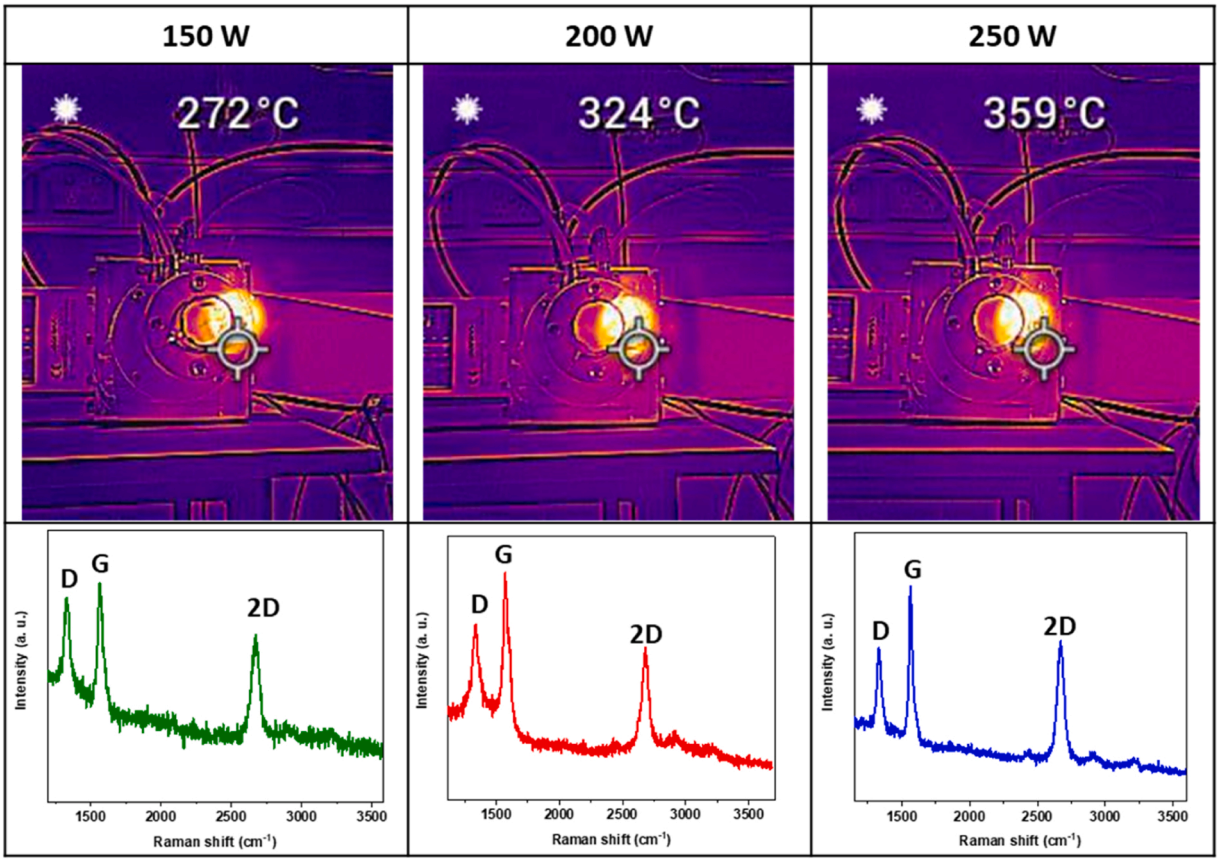

Fig. 3. Temperature profiles during synthesis at various microwave powers and the corresponding Raman spectrum.

2.4. Electrochemical experiment

Cyclic voltammetry (CV) responses of bare and modified GCE were analysed for DA, UA, and AA in 0.1 M phosphate buffer solution (PBS) (pH 7.0). For individual detection, 1 mM solution of each analyte was prepared, whereas, in a simultaneous detection 1 mM of DA and 1 mM of UA were mixed with 5 mM of AA. Following parameters were used for CV measurement; potential range; −200–800 mV, scan rate: 50 mV/sec.

The as-fabricated graphene was examined by Raman spectroscometer using Witec, 532 nm laser instrument. The morphology and transmission electron microscopy (TEM) images were obtained through scanning electron microscope (SEM) (Hitachi SU 5000), and JEOL 2100 F machine respectively. Electrochemical measurements were performed on the potentiostat device (PalmSens 4, Palm Instruments BV, The Netherlands) using 3-electrode system. X-ray diffraction (XRD) was conducted using Bruker, D8-Advance X-ray diffractometer, Cu Kα, $\lambda = 0.154$ nm.

3. Results and discussions

Fig. 3 represents the temperature profiles during synthesis at various microwave powers and the corresponding Raman spectrum. The temperature is measured at the centre of the quartz tube, where the plasma is most intense, resulting in the highest temperature. This hot zone is where graphene synthesis primarily occurs. It is evident that as microwave power increases, the temperature also rises. While the temperature difference may not be significant, it does impact the characteristics of the graphene structure. This is evident in the variations in the D peaks observed in the Raman spectra. The D peak is most pronounced at 150 W, potentially indicating a higher oxygen content. However, there is not a significant difference between the samples synthesized at 200 W and 250 W. Given that 200 W is more energy-efficient, we have considered it as the optimal parameter. Subsequent investigations and discussions are based on the 200 W sample.

Table 1
The Raman peaks designations corresponding to graphene synthesized under different microwave power conditions.

Microwave power (W)	Wave number of D peak (cm^{-1})	Wave number of G peak (cm^{-1})	Wave number of 2D peak (cm^{-1})	I_D/I_G	I_{2D}/I_G
150	1331	1569	2670	0.98	0.95
200	1339	1581	2673	0.87	0.91
250	1336	1576	2671	0.85	0.92

In the Raman of 200 W graphene, there are three typical feature bands, i.e., D, G, and 2D bands. D peak around 1335 cm^{-1} is usually related to the defects or functional groups [24,25], G peak at ~ 1575 cm^{-1} is due to stretch vibration mode [26], and 2D peak ~2675 cm^{-1} is induced by E_{2g} mode [27]. Our graphene sample showed vibrant three peaks (Fig. 3a). The specific peak designations are provided in Table 1. The minimal shifting of the peaks is typically ascribed to strain within the graphene lattice [28]. The correlation of D and 2D peaks with G peak are ascribed to characteristic features in graphene. I_D/I_G gives an indication of defects in graphene. Higher I_D/I_G of 0.87 in our sample reveals the occurrence of either defects and/or functional groups bonded with oxygen. The oxygen presence is due to the ambient conditions for the synthesis of graphene. I_{2D}/I_G along with FWHM is generally linked to the number of layers, provided that its value is above 2 [29]. In our sample, I_{2D}/I_G of 0.91 and FWHM of 68 cm^{-1} indicates the multi-layered graphene. Overall, the samples did not exhibit significant variations in intensity ratio. Therefore, it can be inferred that power does not exert a substantial influence on the

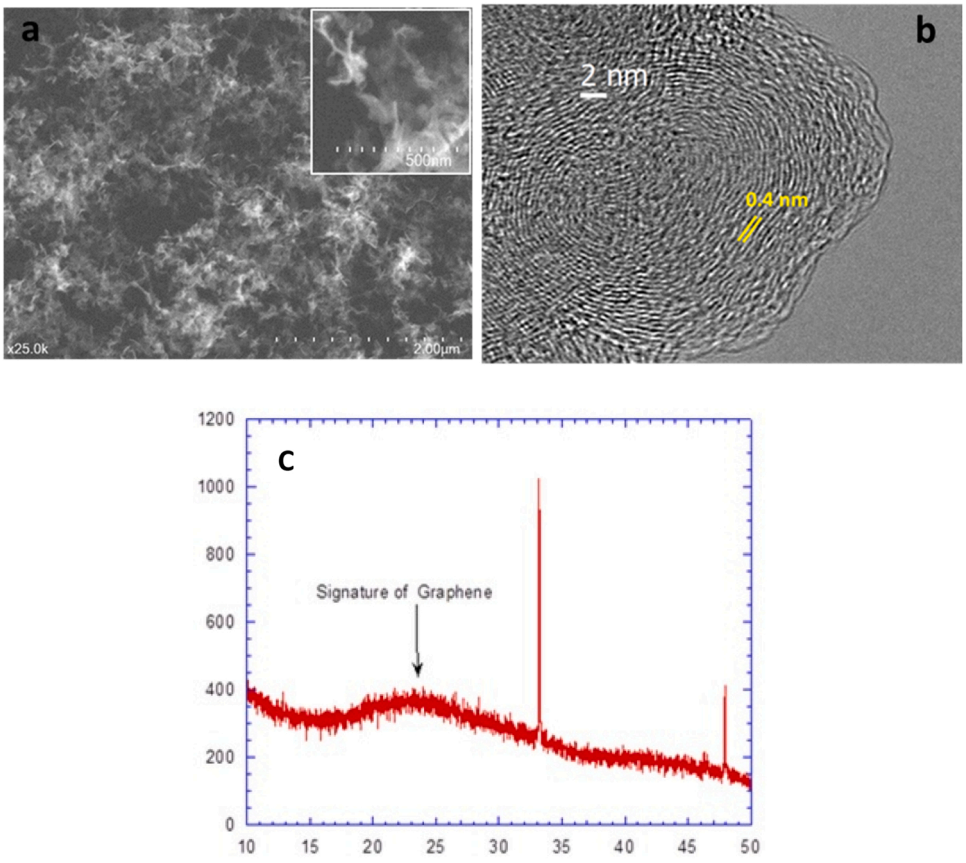

Fig. 4. (a) SEM (b) TEM image and (c) XRD pattern of 200 W graphene synthesized from tea tree oil vapours.

structural properties of graphene. A similar observation was made by Toman *et al.*[30], who associated power with production rate rather than features in the Raman spectrum of graphene.

The TEM images shown in Fig. 4b revealed graphene as a multi-layered. It matches with the interpretation made from I_{2D}/I_G and FWHM analysis. The interlayer spacing of 0.40 nm obtained from TEM images indicates the existence of oxygen functional groups. Thus, it is more likely that the comparatively higher I_D/I_G value in Raman spectrum is because of the existence of oxygen-based functional groups rather than defects or doping [31]. For instance, a study on graphene derived from coconut waste demonstrated that doping could increase the lattice spacings up to 0.36 nm [32]. Therefore, the higher spacings observed in our sample are attributed to oxygen functional groups.

The SEM image in Fig. 4a resembles with the reported images where graphene was synthesized from ethanol [33] or methane [7] in down-stream microwave plasma. The graphene nanosheets have crumbled-paper-like structure, spread randomly on the silicon substrate. Crystalline materials exhibit characteristic XRD patterns that serve as unique fingerprints for material identification. The presence of a distinct peak cantered at $2\theta{=}26.5^{\circ}$, as depicted in Fig. 4c, verifies the successful synthesis of graphene. In another research study, graphene was synthesized from rice husk using a conventional furnace, and it exhibited a comparable XRD diffraction pattern at 26.3°. In contrast to our one-step approach, their process involved the initial synthesis of amorphous carbon. Subsequently, a chemical activation step was employed to transform the amorphous carbon into a crystalline structure, ultimately resulting in the formation of graphene [34].

3.1. Cyclic voltametric detection of dopamine, ascorbic acid, and uric acid

The electrochemical activity of bare GCE and graphene/GCE for concurrent determination of DA, AA, and UA was examined using CV. Overall, it is clear from the Fig. 5 that the peak currents of the modified electrode are significantly greater than bare GCE. We attribute this to the high surface area feature of graphene material.

For DA, the redox peaks were noted at 121 mV and 176 mV, indicating the DA oxidation to o-dopaminequinone and its reduction back to DA [35]. A decreased peak to peak separation between the oxidation and reduction i.e., 55 mV also indicates the superior electrochemical property of graphene/GCE. Moreover, an enhanced anodic peak current of graphene/GCE which is three times higher in comparison with bare GCE, suggests an excellent electrocatalytic behaviour of tea tree-derived graphene modified electrode towards dopamine.

In the instance of UA, a prominent peak of oxidation centred at 263 mV was noted; however, the reduction peak at 194 mV appeared weak. The oxidation peak current of more than two folds higher than the related peak at bare GCE signify the substantial electrocatalytic activity of graphene/GCE towards UA. Similarly, graphene/GCE electrode showed superior performance for AA by increasing anodic peak current (at −16 mV) along with negatively shifting of the peak.

3.2. Simultaneous determination of DA, AA, and UA

CV response of bare and graphene/GCE in ternary mixture is shown in Fig. 6. At the bare GCE only a broad and over-lapped oxidation peak is acquired at 249 mV, and the potentials of biomolecules are indistinguishable. However, at graphene/GCE three sharp and distinct oxidation peaks relating to the oxidation of AA, UA and DA can be observed. The three oxidation peaks for AA, DA and UA are clearly distinguishable at 41 mV, 169 mV and 300 respectively. It can also be observed that peaks are slightly shifted in comparison with individual detection results. Similar phenomenon was observed by Jiao Du et al. [36], where they have attributed it to the different oxidation properties at interface

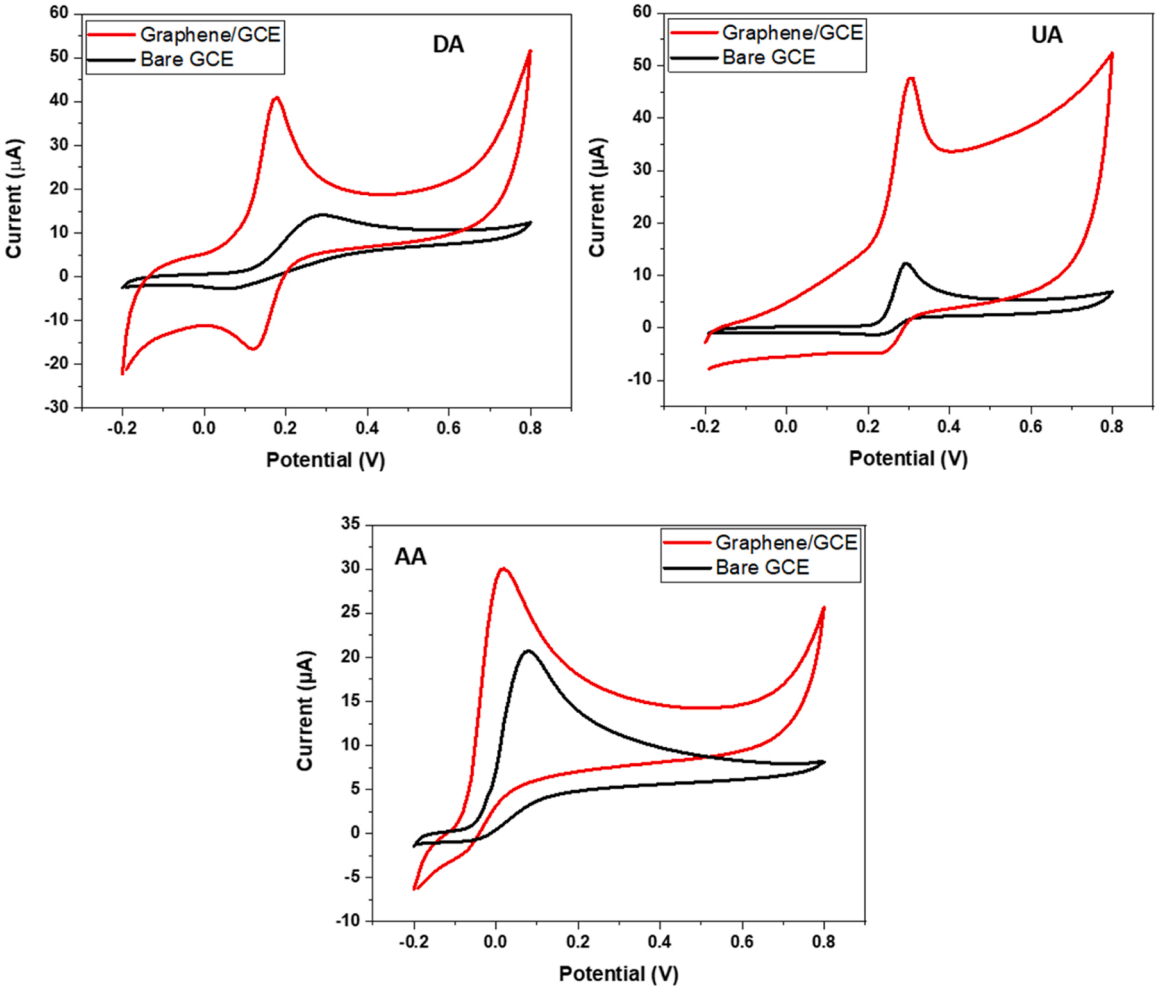

Fig. 5. CV of bare GCE (black), graphene/GCE (red) in 0.1 M PBS (pH 7.0) containing AA (5 mM), DA, and UA (1 mM each). Scan rate: 50 mV/s.

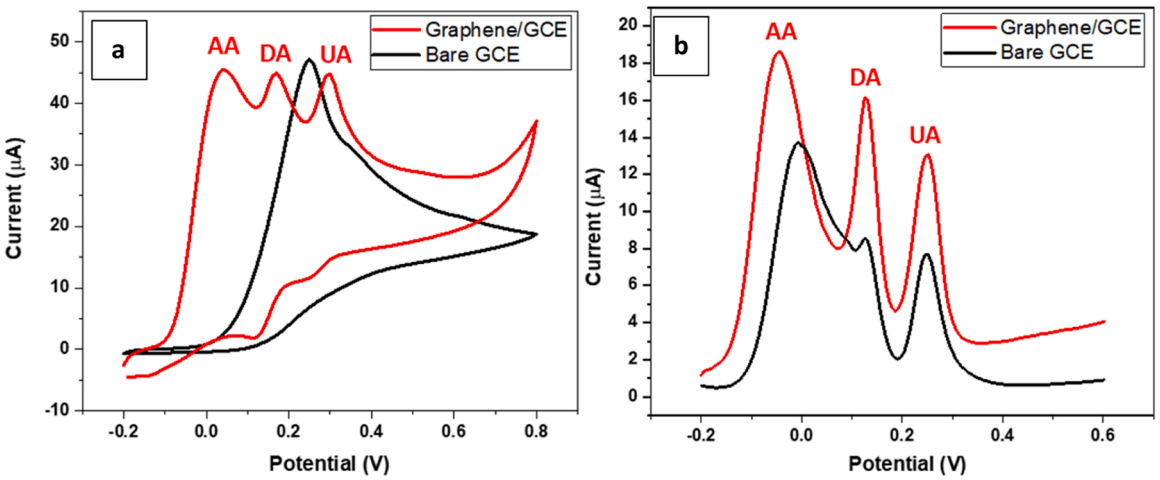

Fig. 6. (a) CV of bare GCE (black), and graphene/GCE (red) in 0.1 M PBS (pH 7.0) containing the mixture of AA (5 mM), DA and UA (1 mM each). Scan rate: 50 mV/s (b) DPV of bare GCE (black), and graphene/GCE (red) in 0.1 M PBS (pH 7.0) containing the mixture of AA (4 mM), DA (0.5 mM), and UA (1 mM). Scan rate 10 mV/sec, amplitude 0.025.

when analytes are adsorbed on the surface of the electrode.

DPV detection of ternary mixture of DA, AA, and UA was performed at bare GCE and graphene/GCE. The electro-oxidation of bare GCE showed three peaks in which AA and DA in particular were indistinct. In contrast, graphene/GCE revealed three peaks of AA, DA, and UA located at −40 mV, 125 mV, and 252 mV respectively. The graphene/GCE peaks are clearly distinguishable and amplified. In this context, we emphasize that the sensing behavior of our pristine graphene is comparable to past studies that utilized complex and expensive composite materials [37,38], such as metal/covalent-organic frameworks [39],

metallic and bimetallic nanoparticles (including precious metals) [40], and artificially synthesized polymers like molecular imprinted polymers [41]. This underscores the simplicity and cost-effectiveness of our approach. Moreover, it demonstrates the significant potential of graphene/GCE for further research into sensitivity and selectivity in the real-time recognition of DA, AA, and UA.

4. Conclusion

This study explored facile, fast, and environmentally friendly method to make graphene using downstream atmospheric pressure microwave plasma. It was demonstrated that *melaleuca alternifolia* vapours could be converted into graphene at comparatively low temperature with the aid of cold plasma. The distinctive D, 2D, and G bands in the Raman spectrum confirmed the graphene's creation. The TEM image revealed a multi-layered graphene structure with interstitial spaces of 0.40 nm. The as-synthesized graphene was drop-casted onto a GCE to test its potential for detecting DA, AA and UA using CV and DPV techniques. The stronger peak currents in individual detection and the accurate detection of the ternary mixture indicated that graphene from tea tree extract has great promise for this application.

In summary, the utilization of a novel graphene synthesis method involving green precursor and cold plasma presents a logical and well-supported alternative to traditional approaches. We highlight the drawbacks of existing methods, emphasizing harsh conditions and extended processing durations. In response, our method employs mild conditions and achieves rapid synthesis within seconds, addressing key concerns associated with conventional techniques. Additionally, we conduct electrochemical tests, demonstrating enhanced current peaks. These findings underscore the potential of the synthesized graphene for applications in electrochemical sensing, suggesting its viability as an alternative to existing therapeutics.

CRediT authorship contribution statement

Yang Liu: Writing – review & editing, Supervision. **Scarlett Allende:** Writing – review & editing, Visualization. **Muhammad Adeel Zafar:** Writing – original draft, Visualization, Investigation, Formal analysis, Data curation. **Mohan V Jacob:** Writing – review & editing, Supervision, Conceptualization.

Declaration of Competing Interest

The authors declare the following financial interests/personal relationships which may be considered as potential competing interests: Mohan Jacob reports was provided by James Cook University. Mohan Jacob reports a relationship with James Cook University that includes:. If there are other authors, they declare that they have no known competing financial interests or personal relationships that could have appeared to influence the work reported in this paper.

Data Availability

Data will be made available on request.

Acknowledgment

M. A. Zafar thankfully acknowledges James Cook University for the financial support through the Australian Government International Research Training Program Scholarship.

References

[1] S. Chakraborty, R. Saha, S. Saha, A critical review on graphene and graphene-based derivatives from natural sources emphasizing on CO(2) adsorption potential. Environ. Sci. Pollut. Res Int (2023).
[2] H. Wang, Q. Fu, C. Pan, Green mass synthesis of graphene oxide and its MnO2 composite for high performance supercapacitor, Electrochim. Acta 312 (2019) 11–21.
[3] S. Bhaskar, et al., Metal-Free, Graphene Oxide-Based Tunable Soliton and Plasmon Engineering for Biosensing Applications, ACS Appl. Mater. Interfaces 13 (14) (2021) 17046–17061.
[4] F. Hadish, et al., Functionalization of CVD grown graphene with downstream oxygen plasma treatment for glucose sensors, J. Electrochem. Soc. 164 (7) (2017) B336.
[5] P. Brisebois, M. Siaj, Harvesting graphene oxide–years 1859 to 2019: a review of its structure, synthesis, properties and exfoliation, J. Mater. Chem. C. 8 (5) (2020) 1517–1547.
[6] C. Melero, et al., Scalable graphene production from ethanol decomposition by microwave argon plasma torch, Plasma Phys. Control. Fusion 60 (1) (2017) 014009.
[7] N. Bundaleska, et al., Large-scale synthesis of free-standing N-doped graphene using microwave plasma, Sci. Rep. 8 (1) (2018) 1–11.
[8] N. Bundaleska, et al., Microwave plasma enabled synthesis of free standing carbon nanostructures at atmospheric pressure conditions, Phys. Chem. Chem. Phys. 20 (20) (2018) 13810–13824.
[9] P. Ekwere, et al., Microwave synthesis of antimony oxide graphene nanoparticles - a new electrode material for supercapacitors, Nanoscale Adv. 5 (18) (2023) 5137–5153.
[10] M.V. Jacob, et al., Catalyst-free plasma enhanced growth of graphene from sustainable sources, Nano Lett. 15 (9) (2015) 5702–5708.
[11] M.A. Zafar, M.V. Jacob, Plasma-based synthesis of graphene and applications: a focused review, Rev. Mod. Plasma Phys. 6 (1) (2022) 37.
[12] N. Murugan, et al., 2D-titanium carbide (MXene) based selective electrochemical sensor for simultaneous detection of ascorbic acid, dopamine and uric acid, J. Mater. Sci. Technol. 72 (2021) 122–131.
[13] S.A. Abrori, et al., Comparison of a 2D/3D imidazole-based MOF and its application as a non-enzymatic electrochemical sensor for the detection of uric acid, N. J. Chem. 46 (44) (2022) 21342–21349.
[14] Ce Zou, et al., Fabrication of reduced graphene oxide-bimetallic PdAu nanocomposites for the electrochemical determination of ascorbic acid, dopamine, uric acid and rutin, J. Electroanal. Chem. 805 (2017) 110–119.
[15] B. Demirkan, et al., Composites of bimetallic platinum-cobalt alloy nanoparticles and reduced graphene oxide for electrochemical determination of ascorbic acid, dopamine, and uric acid, Sci. Rep. 9 (1) (2019) 1–9.
[16] H. Huang, et al., Electrochemical sensor based on a nanocomposite prepared from TmPO4 and graphene oxide for simultaneous voltammetric detection of ascorbic acid, dopamine and uric acid, Microchim. Acta 186 (3) (2019) 1–9.
[17] Y. Wei, et al., Simultaneous detection of ascorbic acid, dopamine, and uric acid using a novel electrochemical sensor based on palladium nanoparticles/reduced graphene oxide nanocomposite, Int. J. Anal. Chem. 2020 (2020).
[18] D. Minta, et al., N-doped reduced graphene oxide/gold nanoparticles composite as an improved sensing platform for simultaneous detection of dopamine, ascorbic acid, and uric acid, Sensors 20 (16) (2020) 4427.
[19] J. Gao, et al., Electrodeposited NiO/graphene oxide nanocomposite: An enhanced voltammetric sensing platform for highly sensitive detection of uric acid, dopamine and ascorbic acid, J. Electroanal. Chem. 852 (2019) 113516.
[20] L. Zhang, et al., Fabrication of electro-active Pt/IMo6O24/graphene oxide nanohybrid modified electrode for the simultaneous determination of ascorbic acid, dopamine and uric acid, J. Electrochem. Soc. 166 (8) (2019) H351.
[21] J. Feng, et al., Electrochemical detection mechanism of dopamine and uric acid on titanium nitride-reduced graphene oxide composite with and without ascorbic acid, Sens. Actuators B: Chem. 298 (2019) 126872.
[22] M.A. Zafar, et al., Plasma-Based Synthesis of Freestanding Graphene from a Natural Resource for Sensing Application, Adv. Mater. Interfaces 10 (11) (2023) 2202399.
[23] M.A. Zafar, M.V. Jacob, Synthesis of free-standing graphene in atmospheric pressure microwave plasma for the oil-water separation application, Appl. Surf. Sci. Adv. 11 (2022) 100312.
[24] J. Ye, et al., Defect formation-induced tunable evolution of oxygen functional groups for sodium storage in porous graphene, Chem. Commun. 56 (7) (2020) 1089–1092.
[25] Zafar, M.A., et al., *Single-Step Synthesis of Nitrogen-Doped Graphene Oxide from Aniline at Ambient Conditions*. ACS Applied Materials & Interfaces, 2022.
[26] W. Fu, X. Zhao, W. Zheng, Growth of vertical graphene materials by an inductively coupled plasma with solid-state carbon sources, Carbon 173 (2021) 91–96.
[27] H. Xu, et al., Properties of graphene-metal contacts probed by Raman spectroscopy, Carbon 127 (2018) 491–497.
[28] Z. Zafar, et al., Evolution of Raman spectra in nitrogen doped graphene, Carbon 61 (2013) 57–62.
[29] H. Kato, N. Itagaki, H. Im, Growth and Raman spectroscopy of thickness-controlled rotationally faulted multilayer graphene, Carbon 141 (2019) 76–82.
[30] J. Toman, et al., On the gas-phase graphene nanosheet synthesis in atmospheric microwave plasma torch: Upscaling potential and graphene nanosheet-copper nanocomposite oxidation resistance. Fuel Process. Technol. 239 (2023) 107534.
[31] M.A. Zafar, et al., Expeditious and Eco-friendly fabrication of Graphene-Ag nanocomposite for methyl paraben sensing, Appl. Surf. Sci. 638 (2023) 158006.
[32] R. Siburian, et al., Coconut waste to green nanomaterial: Large scale synthesis of N-doped graphene nano sheets, Nano-Struct. Nano-Objects 36 (2023) 101061.
[33] J. Toman, et al., On the transition of reaction pathway during microwave plasma gas-phase synthesis of graphene nanosheets: From amorphous to highly crystalline structure, Plasma Process. Polym. (2021) e2100008.

[34] B. Somasekaran, A. Thirunarayanaswamy, I. Palanivel, Green synthesis of clean edge graphene nanosheets using natural precursor, Mater. Plast. 58 (3) (2021).
[35] N. Roy, S. Yasmin, S. Jeon, Effective electrochemical detection of dopamine with highly active molybdenum oxide nanoparticles decorated on 2, 6 diaminopyridine/reduced graphene oxide, Microchem. J. 153 (2020) 104501.
[36] J. Du, et al., Novel graphene flowers modified carbon fibers for simultaneous determination of ascorbic acid, dopamine and uric acid, Biosens. Bioelectron. 53 (2014) 220–224.
[37] A. Aziz, et al., Silver/graphene nanocomposite-modified optical fiber sensor platform for ethanol detection in water medium, Sens. Actuators B: Chem. 206 (2015) 119–125.
[38] A. Eftekhari, et al., Sensitive and selective electrochemical detection of bisphenol A based on SBA-15 like Cu-PMO modified glassy carbon electrode, Food Chem. 358 (2021) 129763.
[39] X.-H. Liang, et al., Metal/covalent-organic frameworks-based electrochemical sensors for the detection of ascorbic acid, dopamine and uric acid, Coord. Chem. Rev. 497 (2023) 215427.
[40] H. Charlton van der, S. Vernon, Nanoparticles Application in the Determination of Uric Acid, Ascorbic Acid, and Dopamine, Russ. J. Electrochem. 58 (5) (2022) 341–359.
[41] G.S. Geleta, Recent advances in electrochemical sensors based on molecularly imprinted polymers and nanomaterials for detection of ascorbic acid, dopamine, and uric acid: a review, Sens. Bio-Sens. Res. 43 (2024) 100610.